

MIT MRAC Based Boost Converter with Modified 2nd-Order Reference Model

Peng Mao^{1, a*}, Weijian Wang¹, Yonghong Zhang¹, Li Zhou¹,

Min Zhang¹, Huafeng Xiao², and Jun Cai¹

¹ C-MEIC & CICAET, Nanjing University of Information Science & Technology, China

²Southeast University, China

^apengmao_nuist@nuist.edu.cn

Keywords: MIT MRAC, reference model, boost converter, voltage control

Abstract. To improve overall performance of Boost converter, MIT model reference adaptive control (MRAC) scheme was used to control the output voltage. Average model of the boost converter was built and the principle of the MIT MRAC was analyzed. Modified 2nd-order model was used as reference model to improve dynamic performance of the system. A new parameter design method for the 2nd-order reference model was proposed. Simulation results verified the voltage control scheme and the parameter design method.

Introduction

Boost converter is widely used in industry field^[1], and the control scheme greatly effects its overall performance. Up to now, proportional-integral (PI) control scheme is the most popular scheme for this kind of converter^[2]. However, this traditional controller also has its own limitations, e.g. the system performance will change with the fluctuation of circuit parameters because controller parameters are fixed usually^[3].

MIT MRAC is one of relatively early adaptive control methods. Ideally, with adaptive law, the system can achieve the same performance with that of reference model^[4]. Although MIT MRAC cannot make sure stability of the system absolutely, it is still a practical adaptive control method for its simplicity and convenience of algorithm implementation, specially, not like stability theory based MRAC methods, MIT MRAC is also suitable for non minimum phase system e.g. boost converter.

Based on above consideration, boost converter with MIT MRAC scheme for voltage control was studied. Modified 2nd-order reference model was used to improve performance of the system. Parameter design method of the reference model was analyzed. Simulation was mde to verify the control scheme in the end.

Modeling of Boost Converter

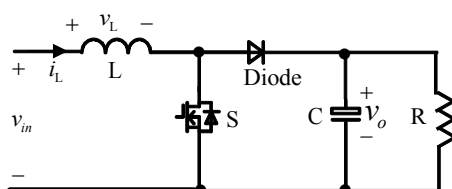


Fig. 1 Topology of boost converter

Topology of boost converter is shown in Fig. 1, v_{in} , v_o are instantaneous voltage, L , C are input and output side filter separately. Suppose switching frequency f_s is high enough, the large signal average model^[2] of the converter can be yield in Eq.1 when the inductor current is continuous

$$\begin{cases} L \frac{d(t)\langle i_L(t) \rangle_{T_s}}{dt} = \langle v_m(t) \rangle_{T_s} - d'(t)\langle v_o(t) \rangle_{T_s} \\ C \frac{d(t)\langle v_o(t) \rangle_{T_s}}{dt} = d'(t)\langle i_L(t) \rangle_{T_s} - \frac{\langle v_o(t) \rangle_{T_s}}{R} \end{cases} \quad (1)$$

Switching period $T_s=1/f_s$, $d(t)$, $d'(t)$ are conduction and close-off duty cycle separately, $\langle i_L(t) \rangle_{T_s}$ is the average inductor current during a switching period, other expressions are defined similarly. Based on Eq.1, time domain small signal model of the system can be deduced as shown in Eq.2, where V_{in} , V_o , I_L and D are steady state value at the moment of t .

$$\begin{cases} L \frac{d\hat{i}_L(t)}{dt} = [\hat{v}_m(t) - D'\hat{v}_o(t) + V_o\hat{d}(t)] \\ C \frac{d\hat{v}_o(t)}{dt} = [D\hat{i}_L(t) - \frac{\hat{v}_o(t)}{R} - I_L\hat{d}(t)] \end{cases} \quad (2)$$

Frequency domain model can be obtained as shown in Eq.3 with Laplace transformation of Eq.2.

$$F_p(s) = \left. \frac{\hat{v}_o(s)}{\hat{d}(s)} \right|_{\hat{v}_{in}(s)=0} = \frac{V_o(1-Ls/(D^2R))}{LCs^2 + D^2} \quad (3)$$

Eq.3 is the key transfer function which will be used to control v_o with MIT MRAC scheme. When v_{in} is 200V, v_o is 400V, L is 1mH, C is 2000uF, R is 10Ω, f_s is 20kHz, the above transfer function F_p can be got shown in Eq.4.

$$F_p(s) = \frac{-0.08s + 200}{0.000002s^2 + 0.0001s + 0.25} \quad (4)$$

Principle of MIT MRAC Controller

Diagram of MIT MRAC is shown in Fig.2, S_r is reference signal, F_p is transfer function of the plant, that is the transfer function from output of controller to the output of the system, F_m is reference model, y_m and y_p are ideal output and real output separately. The object of MRAC is to let $F_c \bullet F_p$ approach F_m by adjusting controller parameters dynamically according to the adaptive law. $k_c(0)$ is the initial value of k_c . μ can be selected as a small constant.

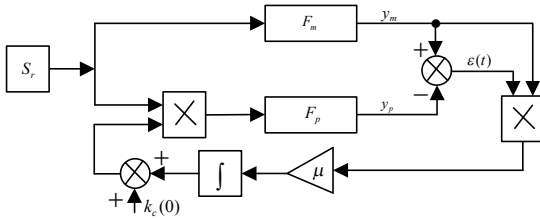


Fig. 2 Control diagram of MIT MRAC

Parameter Design of 2nd-Order Reference Model

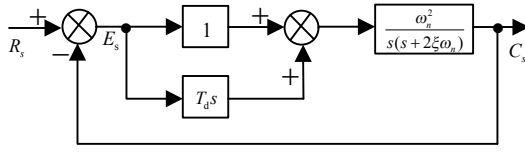


Fig.3 Diagram of modified 2nd-order system

Reference model has significant effect on MRAC system, modified 2nd-order model shown in Fig.3 was used to improve dynamic performance of the system with its differentiation element. Transfer function of the 2nd-order system is shown in Eq.5

$$G(s) = \frac{\omega_n^2}{z} \frac{s + z}{s^2 + 2\xi_d \omega_n s + \omega_n^2} \quad (5)$$

where

$$z = 1/T_d \quad (6)$$

$$\xi_d = \xi + \omega_n / (2z) \quad (7)$$

Similarly as traditional 2nd-order model, rising time t_r , peak value time t_p and overshoot coefficient σ are key index of the system as shown in Eq.8.

$$\left\{ \begin{array}{l} t_r = \frac{-\phi}{\omega_n \sqrt{1 - \xi_d^2}} \\ t_p = \frac{\beta - \phi}{\omega_n \sqrt{1 - \xi_d^2}} \\ \sigma = r \sqrt{1 - \xi_d^2} e^{-\xi_d \omega_n t_p} \times 100\% \end{array} \right. \quad (8)$$

where

$$\left\{ \begin{array}{l} \phi = -\pi + \arctan \left[\omega_n \sqrt{1 - \xi_d^2} / (z - \xi_d \omega_n) \right] + \arctan(\sqrt{1 - \xi_d^2} / \xi_d) \\ \beta = \arctan(\sqrt{1 - \xi_d^2} / \xi_d) \\ r = \sqrt{z^2 - 2\xi_d \omega_n z + \omega_n^2} / z \sqrt{1 - \xi_d^2} \end{array} \right. \quad (9)$$

It can be seen from Eq.8 and Eq.9, t_r , t_p and σ are all transcendental function of T_d , ξ , ω_n . Parameter design method of the modified 2nd-order system will be discussed as follows.

Firstly, T_d should be set properly as shown in Eq.10. The reason for limitation of T_d is that, too small T_d cannot make full use of quick advantage of differentiation element, while the system may become instable if T_d is too large.

$$z = k_z \xi \omega_n \quad k_z \in [2, 5] \quad (10)$$

Combined with Eq.7, the inequality group can be drawn as in Eq.11 (the derivation process can be referred to appendix A)

$$\left\{ \begin{array}{l} \xi_d \geq 0.633 \\ \xi \in \left[\frac{\xi_d - \sqrt{\xi_d^2 - 0.4}}{2}, \frac{\xi_d + \sqrt{\xi_d^2 - 0.4}}{2} \right] \end{array} \right. \quad (11)$$

From Eq.8 it can be seen, ξ_d has significant effect on σ , even though it is not the sole decisive factor. Exponential part dominates σ , which means that σ can keep constant if ξ_d increases meanwhile ω_n decreases. Based on the above analysis and the fact that ω_n is increasing function of ξ (the derivation process can be referred to appendix B), decrease of ξ and increase of ξ_d meanwhile can keep the same σ .

From above analysis, parameter design method suitable for engineering application can be summarized as follows.

- 1) Select ξ_d . To achieve better dynamic performance, ξ_d can be selected at a higher value.
- 2) Calculate the range of ξ with Eq.11. Decrease of ξ benefits for system dynamic performance.
- 3) Select t_r , and substitute t_r into Eq.12, ω_n can be calculated out. The final rising time will be smaller than the selected value because of differential element.

$$t_r = (\pi - \arccos \xi) / (\omega_n \sqrt{1 - \xi^2}) \quad (12)$$

4) Substitute ξ_d, ξ and ω_n into Eq.7 and calculate out z .

5) Substitute ξ_d, ω_n and z into Eq.5 and get the 2nd-order model.

For example, if ξ_d is set to 0.95, the range of ξ will be [0.12, 0.829]. When ξ is selected at 0.2, and t_r is selected at 0.5, ω_n and z will be 3.6 and 2.4 separately. The final 2nd-order model is shown as Eq.13

$$G(s) = (5.4s + 12.96) / (s^2 + 6.84s + 12.96) \quad (13)$$

Simulation Results

Frequency Domain Simulation. Frequency domain simulation was made according to the control diagram shown in Fig.2, where $k_c(0)=0$, $\mu=3 \times 10^{-6}$, plant model and reference model are shown in Eq.4 and Eq.13 separately. Simulation results of y_m and y_p shown in Fig.4 and Fig.5 prove that the reference model and control plant has approximately the same dynamic performance.

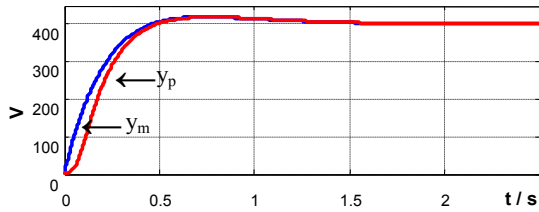


Fig.4 Simulation results of y_m and y_p

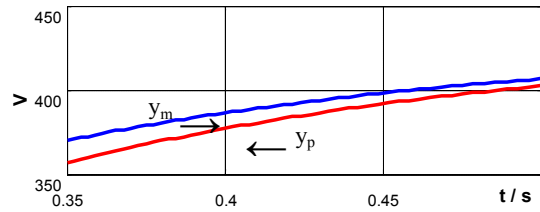


Fig.5 Partial enlarged detail of y_m and y_p

Time Domain Simulation. Time domain simulation results are shown in Fig.6, v_m is the reference of v_{out} . Load resistor R change from 10Ω to 20Ω at 2s. Fig.7 and Fig.8 are partial enlarged detail of v_m and v_{out} . Simulation results show that there is no steady error between v_{out} and v_m although saturation of controller effect tracking at the beginning time. Waveform of v_{out} shown in Fig.8 shows that 50% load decrease only leads to 5% voltage ripple, which verifies MIT MRAC scheme.

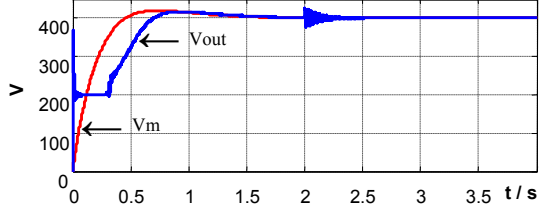


Fig.6 Waveform of v_m and v_{out}

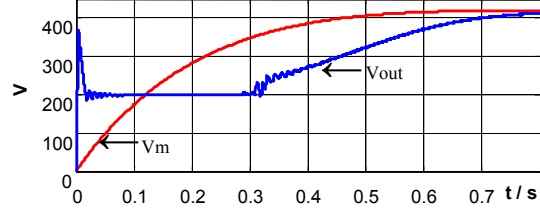


Fig.7 Partial enlarged detail of v_m and v_{out}

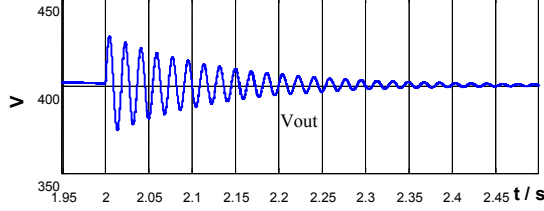


Fig.8 Partial enlarged detail of v_{out}

Conclusions

1) MIT MRAC scheme was used for voltage control of Boost converter, which was verified by simulation results.

2) Modified 2nd-order model was used in the control scheme, and parameter design method for the reference model was proposed.

Appendix A

Substitute Eq.10 into Eq.7, Eq.14 can be got

$$\xi_d = \xi + 1/(2k_z \xi) \quad (14)$$

Arrange Eq.14, we can get Eq.15

$$k_z = 1/(2\xi_d \xi - 2\xi^2) \quad (15)$$

When $k_z \in [2, 5]$, inequality of Eq.16 can be got

$$0.1 \leq \xi_d \xi - \xi^2 \leq 0.25 \quad (16)$$

Rearrange Eq.16, can we get

$$\begin{cases} \xi^2 - \xi_d \xi + 0.1 \leq 0 \\ \xi^2 - \xi_d \xi + 0.25 \geq 0 \end{cases} \quad (17)$$

Take ξ as variable, to ensure establishment of the 1st inequality of Eq.17, Eq.18 should hold

$$\Delta = \xi_d^2 - 0.4 \geq 0 \quad (18)$$

From Eq.18, Eq.19 holds

$$\xi_d \geq 0.633 \quad (19)$$

Substitute Eq.19 into the 2nd inequality of Eq.17, inequality of $\xi > 0$ can be got, which means Eq.19 gives the final range of ξ_d . Take Eq.19 into 1st inequality of Eq.17, Eq.20 can be got.

$$\xi \in \left[\frac{\xi_d - \sqrt{\xi_d^2 - 0.4}}{2}, \frac{\xi_d + \sqrt{\xi_d^2 - 0.4}}{2} \right] \quad (20)$$

Appendix B

From Eq.12, Eq.21 can be got

$$\omega_n = (\pi - \arccos \xi) / (t_r \sqrt{1 - \xi^2}) \quad (21)$$

In Eq.21, t_r is constant and ξ is variable, take derivation of Eq.21, can we get Eq.22

$$\frac{d\omega_n}{d\xi} = [1 + \xi (\pi - \arccos \xi) / \sqrt{1 - \xi^2}] / [t_r (1 - \xi^2)] \quad (22)$$

When $0 < \xi < 1$, Eq.22 >0 always holds, which proves that ω_n is increasing function of ξ .

Acknowledgment

This research is sponsored by “National Natural Science Foundation of China (No. 51407203)” and “Laboratory Opening Project of C_MIEC(No. KCMEIC01) ”.

References

- [1] B. Singh, B.N. Singh, IEEE Transactions on Industrial Electronics, 2004, 51(3): 641-660.
- [2] Robert W. Erickson , D. Maksimovic. Fundamentals of power electronics- 2nd edition. Springer, 2001.
- [3] A. Xiong, Y.K. Fan. Application of a PID controller using MRAC techniques for control of the DC electromotor drive[C], IEEE International Conference on Mechatronics and Automation, 2007, August 5-8, Harbin, China: 2616-2621.
- [4] Daniel E. Miller, Nagmeh Mansouri, IEEE Transactions on Automatic Control, 2010, 55(9):2014-2029.